PROCEEDINGS, 43rd Workshop on Geothermal Reservoir Engineering
Stanford University, Stanford, California, February 12-14, 2018
SGP-TR-213

Microearthquake Hypocenter-Location and Focal-Mechanism Inversions for the EGS Collab Project: A Synthetic Study

Yu Chen, Lianjie Huang, and EGS Collab Team[1]

Los Alamos National Laboratory, Los Alamos, NM, 87545, USA

chenyu@lanl.gov; ljh@lanl.gov

Keywords: anisotropic media, enhanced geothermal systems, focal mechanism, hydraulic fracturing, hypocenter location, microearthquake, moment tensor, monitoring well.

ABSTRACT

Multiple U.S. national laboratories and universities are conducting collaborative research under the EGS Collab project supported by the U.S. Department of Energy, to understand the fracture creation and imaging during fracturing in enhanced geothermal systems. Microearthquake hypocenter locations and focal mechanisms will be used to monitor hydraulic fracturing growth and characterization at the EGS Collab experimental site at the Stanford Underground Research Facility using geophones in multiple monitoring wells. To design a geophone network for cost-effective passive seismic monitoring, we conduct numerical simulations to study the relationship between geophone distributions and standard deviation errors of microearthquake hypocenter locations, and that between geophone distributions and focal-mechanism inversion errors. Our results indicate that microearthquake hypocenter locations and focal mechanisms can be reasonably well reconstructed for the EGS Collab Experiment 1 using the current design of six monitoring wells, including four fracture-parallel monitoring wells and two orthogonal wells. Eight geophones evenly distributed in four parallel monitoring wells or twelve geophones in all six monitoring wells are required for hypocenter location, and twelve geophones evenly distributed in six wells or sixteen geophones in four wells are needed for focal-mechanism inversion.

1. INTRODUCTION

Enhanced geothermal systems (EGS) generate geothermal electricity without the need for natural convective hydrothermal resources. When natural cracks and pores do not achieve economic flow rates, stimulation could be used in EGS to create fractures and enhance the permeability. EGS technologies enhance and/or create geothermal resources through hydraulic stimulation. It is important to understand how the rock mass responses to hydraulic stimulation and how the permeability change throughout the EGS development, for achieving commercial viability of EGS.

The Department of Energy's Geothermal Technologies Office (GTO) funded national laboratories and universities to focus on GTO's vision for longer-term, transformational enhanced geothermal systems (EGS). The EGS Collab project was established as a collaborative experimental and model comparison initiative, to address critical and fundamental barriers to EGS advancement by facilitating direct collaboration between the geothermal reservoir modeling community, experimentalists, and geophysicists in developing and implementing characterization and development, monitoring, and stimulation methods. The EGS Collab provides the opportunities for reservoir model prediction and validation, in coordination with in depth analysis of geophysical and other fracture characterization data with an ultimate goal of understanding the basic relationship among stress, seismicity and permeability enhancement (Dobson et al., 2017; Kneafsey et al., 2018).

The project has initiated a field experiment at the Stanford Underground Research Facility (SURF) site located in Lead, South Dakota, at the former site of the Homestake Gold Mine. The experiment is within a drift located approximately 1.5 km beneath the surface. The project has drilled an injection well (green cylinder in Figure 1) and a production well (red cylinder in Figure 1) and plans to create two fractures (blue circles in Figure 1) with the diameters of approximately 10-20 m. The experiment has drilled six monitoring wells (yellow cylinders in Figure 1), including four wells (PST, PSB, PDT and PBT in Figure 1) parallel to, and two wells (OT, OB in Figure 1) orthogonal to the two potential fractures. The geophones (illustrated by black spheres in Figure 1) will be deployed within those monitoring wells. The distances among the fracture planes and the parallel monitoring wells are about 5 m.

---

[1]J. Ajo-Franklin, S.J. Bauer, T. Baumgartner, K. Beckers, D. Blankenship, A. Bonneville, L. Boyd, S.T. Brown, J.A. Burghardt, T. Chen, Y. Chen, C. Condon, P.J. Cook, P.F. Dobson, T. Doe, C.A. Doughty, D. Elsworth, J. Feldman, A. Foris, L.P. Frash, Z. Frone, P. Fu, K. Gao, A. Ghassemi, H. Gudmundsdottir, Y. Guglielmi, G. Guthrie, B. Haimson, A. Hawkins, J. Heise, C.G. Herrick, M. Horn, R.N. Horne, J. Horner, M. Hu, H. Huang, L. Huang, K. Im, M. Ingraham, T.C. Johnson, B. Johnston, S. Karra, K. Kim, D.K. King, T. Kneafsey, H. Knox, J. Knox, D. Kumar, K. Kutun, M. Lee, K. Li, R. Lopez, M. Maceira, N. Makedonska, C. Marone, E. Mattson, M.W. McClure, J. McLennan, T. McLing, R.J. Mellors, E. Metcalfe, J. Miskimins, J.P. Morris, S. Nakagawa, G. Neupane, G. Newman, A. Nieto, C.M. Oldenburg, W. Pan, R. Pawar, P. Petrov, B. Pietzyk, R. Podgorney, Y. Polsky, S. Porse, S. Richard, M. Robertson, B. Roggenthen J. Rutqvist, H. Santos-Villalobos, P. Schwering, V. Sesetty, A. Singh, M.M. Smith, H. Sone, C.E. Strickland, J. Su, C. Ulrich, A. Vachaparampil ,C.A. Valladao, W. Vandermeer, G. Vandine, D. Vardiman, V.R.. Vermeul, J.L. Wagoner, H.F. Wang, J. Weers, J. White, M.D. White, P. Winterfeld Y.S. Wu, Y. Wu, Y. Zhang, Y.Q. Zhang, J. Zhou, Q. Zhou, M.D. Zoback

Microearthquake (MEQ) location and focal mechanism can be used to monitor fracture growth and geomechanical deformation. We recently studied the relationships between standard deviation errors of MEQ locations within a fracture plane and geophone distribution within multiple monitoring wells. The geophones were evenly distributed within two parallel, two orthogonal, four parallel, four orthogonal and six combined wells, respectively. Our study indicated that eight geophones are required for event-location monitoring using noise-free data, while twelve geophones are required using noisy data. The combination of parallel and orthogonal wells does not help with MEQ event location (Huang et al., 2017).

In this paper, we evaluate the optimal network design for microseismic event-location monitoring with the MEQs on two fracture planes and geophone distributions. We further study the network design for focal-mechanism inversion of MEQ data. We use 162 MEQs evenly distributed within two fracture planes shown in blue in Figure 1. The distance between MEQs along each axis of the Cartesian coordinate is 2 m. We evaluate two scenario of geophone distributions, including four parallel wells and all six wells drilled for the project. The geophones evenly distributes in the range of 35 m within the wells and around the center of the fractures (Figure 1). We study the relationships between geophone distributions and MEQ hypocenter-location uncertainty (standard deviation errors), and that between geophone distributions and focal-mechanism inversion uncertainty.

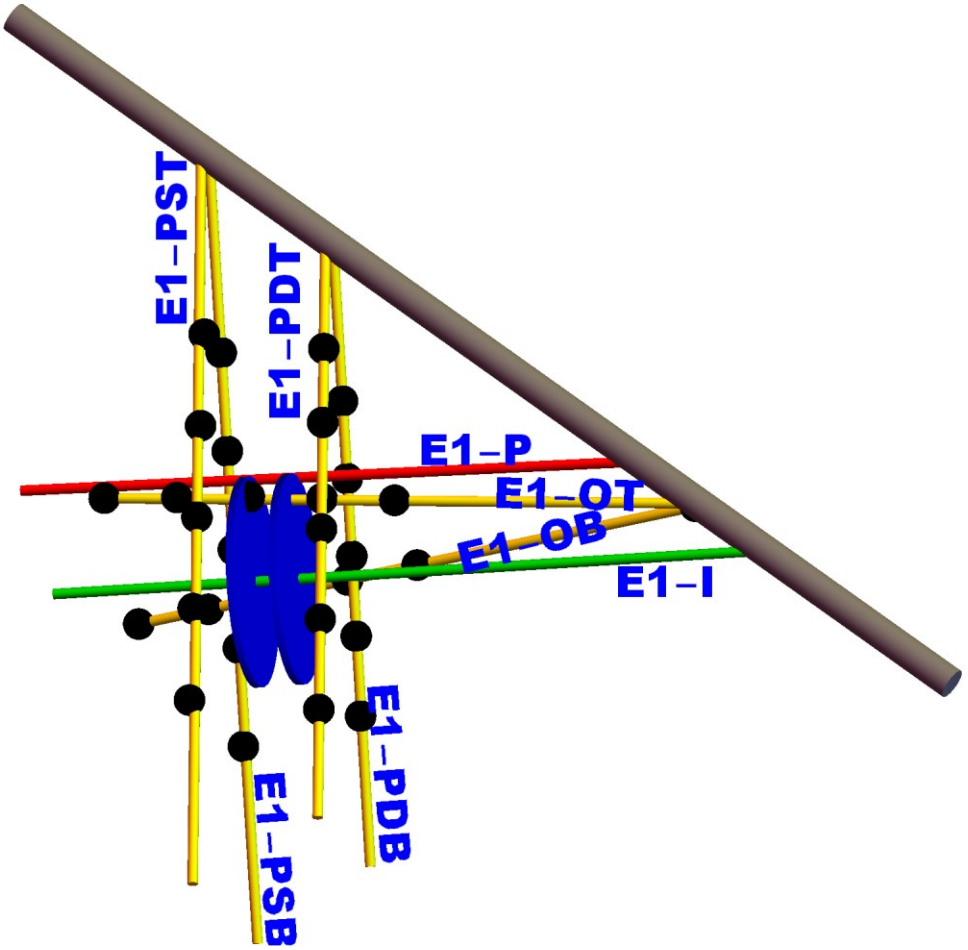

Figure 1: Schematic illustration of monitoring wells at SURF for the EGS Collab Experiment 1. The monitoring wells drilled from the drift (gray cylinder) are in yellow. The injection well is green, and the production well is red. The circular region in blue is the fractures to be created by hydraulic stimulations. The geophones (black spheres) are distributed within the monitoring wells in yellow to monitor induced MEQs evenly distributed within the created fractures in the blue circular regions.

2. DESIGN OF OPTIMAL SEISMIC NETWORK FOR MEQ EVENT-LOCATION MONITORING

We develop a method to examine the hypocenter-location uncertainty for an MEQ event and geophone distribution. The method computes P- and S-wave travel times for a synthetic event to geophones, and then inverts hypocenter location for the synthetic event. The hypocenter-location uncertainty is defined as the standard deviation error of the event location.

We develop an analytical method to calculate travel-time arrivals in homogeneous and anisotropic medium. For the vertical transverse isotropic (VTI) medium, we set the P-wave velocities along the fast and slow axes to be 6.5 km/s and 4.8 km/s, the S-wave velocities along the fast and slow axes to be 4.3 km/s and 3.3 km/s, and the density to be 2.85 x 10^3 kg/m^3 (Huang, et al. 2017). We calculate the stiffness matrix C_{ij} in the VTI medium as follows:

$$C = \begin{bmatrix} 120.4125 & 58.3395 & -29.1698 & 0 & 0 & 0 \\ & 120.4125 & -29.1698 & 0 & 0 & 0 \\ & & 65.664 & 0 & 0 & 0 \\ & & & 52.6965 & 0 & 0 \\ & & & & 52.6965 & 0 \\ & & & & & 31.0365 \end{bmatrix}.$$

We then adopt the Kelvin-Christoffel equation to estimate the slowness of the P and S waves in the specific direction (Carcione, 2007). The slowness can be used to obtain the P- and S-wave arrival times for any locations in this homogeneous, anisotropic medium.

We perform a non-linear inversion to obtain MEQ locations using P- and S-wave travel times. The inversion method adopts a simulated heat-annealing algorithm (Chen et al., 2014) to search for the best hypocenter location for a given event. The method minimizes the least-squares misfits between the predicted and observed P- and S-wave arrival times.

We study the relationships between MEQ hypocenter uncertainty and geophone distributions for the EGS Collab Experiment 1 (Figure 1). Figure 2a exhibits the relationships between standard deviation errors of MEQ hypocenter locations and the total numbers of geophones evenly distributed within the four parallel (red curves) and all six monitoring wells (blue curves), respectively. The results indicate that eight geophones are required in four wells, while twelve geophones are needed in six wells to reach a reasonably small hypocenter uncertainty using noise-free travel-time picks. That is, two geophones in each well are needed for event location. These results are consistent with our previous results (Huang et al., 2017).

Figure 2b exhibits the same inversion but using noisy travel-time picks, which have a Gaussian distribution with a standard deviation of $5x10^{-5}$ seconds. Twelve geophones are required in either four or six wells. The uncertainty further decrease slightly as the number of geophone increase, because increasing the number of geophones statistically reduces the effect from random noise of travel-time picks. The result demonstrates that the combination of parallel and orthogonal wells does not help for MEQ event location.

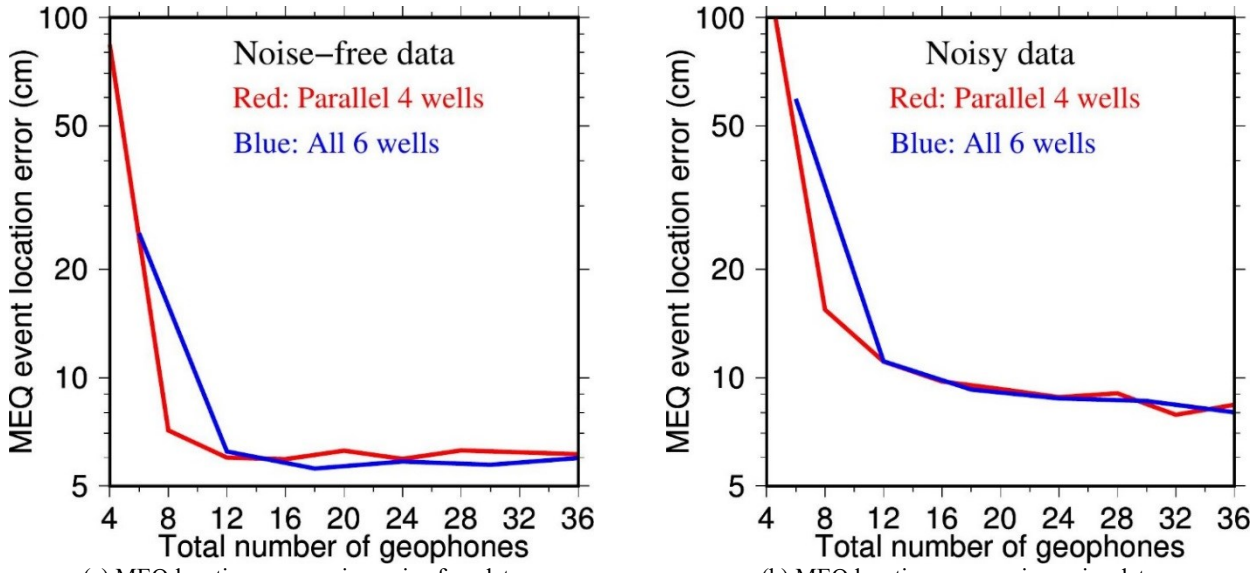

(a) MEQ location errors using noise-free data (b) MEQ location errors using noisy data

Figure 2: Standard deviation errors of MEQ event locations vs. the total numbers of geophones evenly distributed within four parallel (red curves) and all six (blue curves) monitoring wells as shown in Figure 1, for (a) noise-free travel-time picks and (b) noisy travel-time picks.

3. DESIGN OF OPTIMAL SEISMIC NETWORK FOR MEQ FOCAL-MECHANISM INVERSION

We develop a focal-mechanism inversion method to study MEQ focal-mechanism inversion uncertainty for an MEQ source and geophone configuration. Full moment tensor can be decomposed as strike, dip, rake for the double-couple component of focal mechanisms, ISO (isotropic component) and compensated linear vector dipole (CLVD) for the non-double-couple component of focal mechanism, and seismic moment. Double-couple component would exhibit the fault geometry, while non-double-couple component can reveal crack

opening. Here, we adopt seven parameters to represent each event, including strike, dip, rake, ISO, CLVD, and source duration and moment.

We calculate Green's functions using an anisotropic finite-difference waveform modeling method (Gao and Huang, 2017), based on the same velocity/stiffness model adopted in Section 2. The synthetics are the combination of the Green's functions based on the focal mechanism, and then convolved with source duration and moment. We generate synthetic data using given source parameters. We invert for the seven source parameters using the simulated heat-annealing algorithm (Chen et al., 2014) to minimize the misfit between the synthetic data and the predicted synthetics.

We study the relationships between MEQ focal-mechanism standard deviation errors and geophone distribution configurations within four parallel and all six monitoring wells for the EGS Collab Experiment 1 (Figure 1). The geophone distribution configuration is the same as that in Section 2. To simplify the comparison, we define the MEQ double-couple error as the average of strike, dip and slip standard deviation errors, MEQ non-double-couple error as the average of ISO and CLVD standard deviation errors, and MEQ focal-mechanism error as the average of strike/360, dip/90, rake/360, ISO, and CLVD/0.5.

Figure 3a displays the relationships between MEQ focal-mechanism errors and the total numbers of geophones evenly distributed within four parallel and all six monitoring wells, respectively. Twelve geophones in six wells (blue curve in Figure 3a) or sixteen geophones in four wells (red curve in Figure 3a) are required for reliable focal-mechanism inversion.

In Figure 3b, we show the inversion results for synthetic data with 20% white noise. Eighteen geophones in six wells or twenty in four wells are needed for noisy data. Figures 3a and 3b indicates that using all six wells improves capability of recovering focal mechanism when the geophone number is less than sixteen. However, the two scenarios work equally well when the geophone number is more than sixteen. We note that standard deviation errors still decrease as the geophone number increase. For cost-effective monitoring, we suggest that using twelve geophones evenly distributed in all six wells is the optimal design.

We also plot the relationships between double-couple component of MEQ focal-mechanism errors and the total number of geophones in Figures 4a and 4b, and that between non-double-couple component errors and the total number of geophones in Figures 5a and 5b. We obtain similar conclusions as in Figures 3a and 3b. Our optimal network can acquire double-couple error as low as 0.4° and non-double-couple error as low as 0.005.

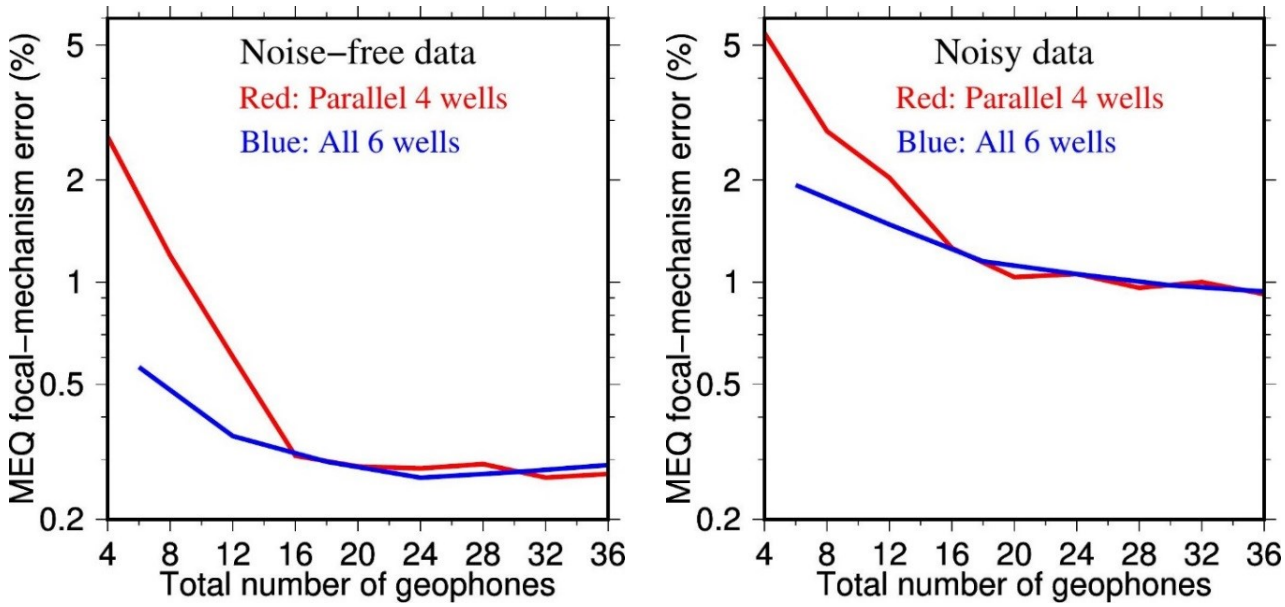

(a) MEQ location errors using noise-free data (b) MEQ location errors using noisy data

Figure 3: Standard deviation errors of MEQ focal mechanisms vs. the total numbers of geophones evenly distributed within four parallel (red curves) and all six (blue curves) monitoring wells as shown in Figure 1, for (a) noise-free synthetic data and (b) noisy synthetic data.

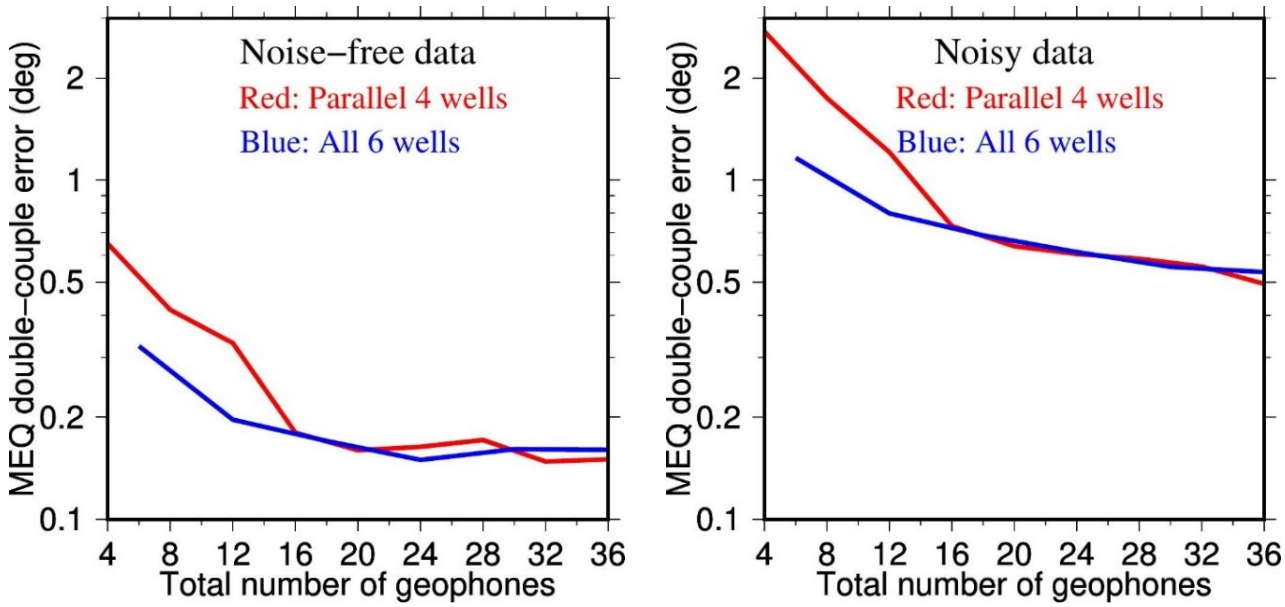

(a) MEQ location errors using noise-free data (b) MEQ location errors using noisy data

Figure 4: Standard deviation errors of double-couple components of MEQ focal mechanisms vs. the total numbers of geophones evenly distributed within four parallel (red curves) and all six (blue curves) monitoring wells as shown in Figure 1, for (a) noise-free synthetic data and (b) noisy synthetic data.

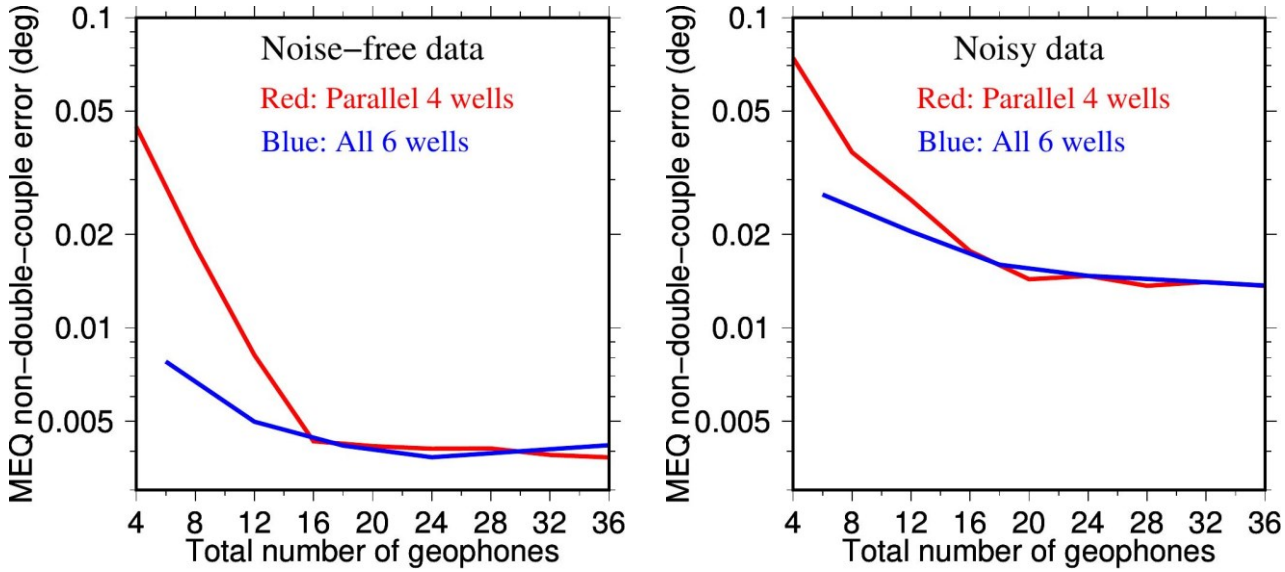

(a) MEQ location errors using noise-free data (b) MEQ location errors using noisy data

Figure 5: Standard deviation errors of non-double-couple components of MEQ focal mechanisms vs. the total numbers of geophones evenly distributed within four parallel (red curves) and all six (blue curves) monitoring wells as shown in Figure 1, for (a) noise-free synthetic data and (b) noisy synthetic data.

4. CONCLUSIONS

We have developed MEQ hypocenter-location and focal-mechanism inversion methods, and performed the resolution tests to study MEQ hypocenter-location and focal-mechanism uncertainties for the two scenarios of source and geophone configurations for the EGS Collab Experiment 1 at SURF. One scenario is to use four parallel monitoring wells, and the other is to use all six monitoring wells. Our numerical study demonstrates that eight geophones evenly distributed in four parallel monitoring wells or twelve geophones in all six monitoring wells are required for hypocenter location, and twelve geophones evenly distributed in six wells or sixteen geophones in four wells are needed for focal-mechanism inversion. More geophones would help reduce the inversion uncertainty caused by random noise.

ACKNOWLEDGEMENTS

This material was based upon work supported by the U.S. Department of Energy, Office of Energy Efficiency and Renewable Energy (EERE), Office of Technology Development, Geothermal Technologies Office, under Award Number DE-AC52-06NA25396 to Los Alamos National Laboratory (LANL). We thank Timothy Kneafsey of LBNL for his careful review of the paper. The United States Government retains, and the publisher, by accepting the article for publication, acknowledges that the United States Government retains a non-exclusive, paid-up, irrevocable, world-wide license to publish or reproduce the published form of this manuscript, or allow others to do so, for United States Government purposes. The computation was performed using super-computers of LANL's Institutional Computing Program.

REFERENCES

Carcione, José M. "Wave fields in real media: Wave propagation in anisotropic, anelastic, porous and electromagnetic media." Vol. 38. Elsevier, (2007).

Chen, Y., Wen, L. and Ji. C., "A cascading failure during the 24 May 2013 great Okhotsk deep earthquake." *Journal of Geophysical Research: Solid Earth,* **119**, (2014), 3035-3049.

Dobson, P., Kneafsey, T.J., Blankenship, D., Valladao, C., Morris, J., Knox, H., Schwering, P., White, M., Doe, T., Roggenthen, W., Mattson, E., Podgorney, R., Johnson, T., Ajo-Franklin, J., and EGS Collab Team, "An Introduction to the EGS Collab SIGMA-V Project: Stimulation Investigations for Geothermal Modeling Analysis and Validation," GRC Transactions, 41, (2017), 837-849.

Gao, K., and Huang, L., "An improved rotated staggered-grid finite-difference method with fourth-order temporal accuracy for elastic-wave modeling in anisotropic media." Journal of Computational Physics, 350, (2017), 361-386.

Huang, L., Chen, Y., Gao, K., Fu, P., Morris, J., Ajo-Franklin, J., Nakagawa, S., and EGS Collab Team, "Numerical modeling of seismic and displacement-based monitoring for the EGS Collab Project." GRC Transaction, 41, (2017), 893-909.

Kneafsey, T.J., Dobson, P., Blankenship, D., Morris, J., Knox, H., Schwering, P., White, M., Doe, T., Roggenthen, W., Mattson, E., Podgorney, R., Johnson, T., Ajo-Franklin, J., Valladao, C., and the EGS Collab team: An Overview of the EGS Collab Project: Field Validation of Coupled Process Modeling of Fracturing and Fluid Flow at the Sanford Underground Research Facility, Lead, SD, *PROCEEDINGS*, 43rd Workshop on Geothermal Reservoir Engineering, Stanford University, Stanford, California, SGP-TR-213 (2018).